Journal of Photochemistry & Photobiology, B: Biology 166 (2017) 232–238

Contents lists available at ScienceDirect

Journal of Photochemistry & Photobiology, B: Biology

journal homepage: www.elsevier.com/locate/jphotobiol

Spontaneous photon emission: A promising non-invasive diagnostic tool for breast cancer

Xiaolei Zhao [a], Jingxiang Pang [a,b], Jialei Fu [c], Yong Wang [d], Meina Yang [b], Yanli Liu [c], Hua Fan [c], Liewei Zhang [c], Jinxiang Han [a,b,*]

[a] Department of Biochemistry and Molecular Biology, Shandong University, Jinan 250012, China
[b] Shandong Medicinal Biotechnology Center, Key Laboratory for Biotech-Drugs of the Ministry of Health, Shandong Academy of Medical Sciences, Jinan 250062, China
[c] Shandong Academy of Traditional Chinese Medicine, Jinan 250355, China
[d] Department of Neurosurgery, Shandong Cancer Hospital, Jinan 250117, China

ARTICLE INFO

Article history:
Received 11 November 2016
Accepted 12 December 2016
Available online 14 December 2016

Keywords:
Spontaneous photon emission (SPE)
Breast cancer
Preliminary screening
Cluster analysis
Oxidative metabolic
Reactive oxygen varieties (ROS)

ABSTRACT

Ultra-weak photon emission (UPE) has attracted significant scientific attention for its potential to monitor the physiological and pathological characteristics of living systems. In this study, we investigated the strength of spontaneous photon emission (SPE) from the right (R) and left (L) side of body surface of human breast cancer-bearing nude mice models, considering the entire breast cancer growth process, and healthy controls using a photon detector. And then we calculated the ratio of the average SPE strength (ratio (R/L)) between the right and left side of each mouse. Cluster analysis was used to evaluate the accuracy rates of strength-R, strength-L, ratio (R/L) and their combination to identify tumor mice from the controls. Our results revealed that the discriminating powers of different parameters were different in different growth stages of tumor: in tumor incubation period, the accuracy rates of strength-R, strength-L, ratio (R/L) and their combination to identify tumor mice from control mice were 63.6%, 40.9%, 81.8% and 86.4%, respectively; For nude mice with tumor diameter <0.5 cm, the accuracies were 72.7%, 45.5%, 86.4% and 90.9%; and for nude mice with tumor diameters larger than 1.5 cm, the accuracies were 86.4%, 77.3%, 95.5% and 100%, respectively. These results indicated that the SPE from the body surface of the lesion site could significantly distinguish tumor mice from the controls when tumors were obvious or when there were no obvious morphological changes, although the accuracy was relatively low. The results suggest that SPE, as a sensitive and promising optical method, may contribute to the preliminary screening of breast cancer, especially for early diagnosis, and it may play a critical role in curtailing the effects of breast cancer and improving the survival of patients in the future.

1. Introduction

All living things spontaneously emit ultra-weak photon emission (UPE), often called biophotons, mainly in the visible region [1]. Spontaneous ultra-weak photon emission (SPE) is an intrinsic attribute of biological systems originating from the relaxation of electronically excited species formed in biological systems during normal or abnormal oxidative metabolic processes [2,3]. Oxidative metabolic processes are the fundamental chemical reactions that sustain life in biological systems, and small changes in living organisms cause changes in metabolism, leading to changes in SPE. Therefore, SPE has many unusual features. It can reflect the overall physiological and pathological conditions of living organisms. As a result, the measurement of SPE as a novel and non-invasive method has attracted considerable attention in monitoring the state of living organism and has been used in many fields, such as agriculture [4,5], detection of food quality [6], evaluation of medicinal properties of herbs [7], assessment of cancer cells or tissues [8–11] and some other health problems [12–16].

Breast cancer is the most common type of cancer in women worldwide and presents the greatest health care challenge in today's world. Despite the vast knowledge of the disease, its incidence has never shown a declining trend. If it can be detected and diagnosed in a nearly stage, breast cancer is one of the most treatable forms of cancer. Thus, early detection and diagnosis is the best way to curtail the effects of this disease and to improve patient survival. Currently, the imaging methods under development for the early diagnosis of breast cancer include ultrasound, X-ray mammography and magnetic resonance imaging. Although the three techniques can provide high spatial resolution, relatively little information about the molecular-level changes of the breast tissue is provided [17–19]. In addition, it is difficult to detect abnormal lesions before morphological characteristics are obvious. For example, according to the National Cancer Institute, up to 10% of all breast

* Corresponding author at: Department of Biochemistry and Molecular Biology, Shandong University, Jinan 250012, China.
E-mail address: samshjx@sina.com (J. Han).

http://dx.doi.org/10.1016/j.jphotobiol.2016.12.009
1011-1344/

cancers, approximately 20,000 cases per year in the United States, fail to be discovered by X-ray mammography [20]. Additionally, X-ray mammography uses ionizing radiation, which has a killing effect on normal somatic cells. Therefore, X-ray mammography should not be used in early medical screening for normal people <35 years old, and X-raymammography should not be performed >1 time per year. Accordingly, it is of great significance to develop a novel detection method as an aid and supplementary diagnostic tool for preliminary screening that is not only non-invasive but also is of sufficient sensitivity and provides some metabolism information about the physiological and pathological conditions of the breast tissue. It is in this setting of the diagnostic dilemma of breast diseases that SPE may have potential.

There are many reports on the relationship between biophoton emission and human cancer. For example, by measuring SPE during human carcinoma cell culture proliferation, Motohiro Takeda et al. found that the intensity of SPE mainly depended on the cell population, and they suggested that SPE had a potential role in cancer diagnosis [21]. Hwan-Wook Kim et al. measured biophoton emission from human cancerous lung tissue and adjacent normal lung tissue and found that biophoton emission could be used to differentiate the tumor from adjacent normal tissue and also showed a salient difference between squamous cell carcinoma and adenocarcinoma [9]. Serum samples were successfully used by Chen et al. to distinguish patients with acute lymphoblastic leukemia from healthy volunteers [12]. In addition, a comparison was performed by Jungdae Kim et al. in 2006 between the intensities of biophoton emission from tumor-bearing mice transplanted with ovarian cancer cells and control mice, and the difference was significant [22]. These studies demonstrated that the measurement of SPE could be considered as a novel and promising optical method for the diagnosis of cancer.

However, most studies focused on tumor cells, tissues or sera and few studies investigated the changes in biophoton emission from the surface of subjects with cancer compared to healthy subjects. In addition, there are no reports on the characteristics of biophoton emission from the body surface of abnormal lesions before morphological characteristics were obvious. Therefore, we conducted research based on previous reports to investigate on the characteristics of SPE from the body of a human breast cancer-bearing nude mouse model, considering the overall growth process (from transplantation into nude mice to growth into a large tumor) of breast cancer using a sensitive photomultiplier tube (PMT). By comparing and analyzing the data, an interesting and meaningful result was found: SPE not only was used to distinguish tumor mice from the health ones but also could be used to predict the occurrence of tumors, even without an obvious morphological change. These results indicated that SPE measurement may play a critical role in preliminary breast cancer screening or at least be a novel, non-invasive, supplementary method for the early diagnosis.

2. Materials and Methods

2.1. SPE-Detection System

The schematic representation of the SPE-detection system used in our study is shown in Fig. 1. The main components of this system include a PMT, PMT housing for cooling, high voltage power supply, shutter system, photon-counting unit, sample stage, moveable frame, control box and a computer with photon-counting software. The control box and computer are placed in the operation room to facilitate tester operation, and the remaining parts of the system are placed in a special darkroom to ensure magnetic and light shielding. As the core component of the detection system, the PMT (ET Enterprises, Britain, 9235QA) is installed on a moveable frame. In this way we can conveniently adjust the detection position of the nude mice and ensure the distance between the detection site and the PMT window is the same for all measurements. A shutter system is placed in front of the PMT to eliminate the disturbance of external light.

SPE from the nude mice was detected by the highly sensitive and low-noise PMT in single-photon-counting mode with a spectral response ranging from 290 nm to 630 nm. The photons were processed by the photon-counting unit and fed into the computer with photon-counting software. To increase the sensitivity and decrease the dark current, the PMT was cooled to −23 °C using FACT50 PMT cooling housing (ET Enterprises, Britain). A sample holder was placed in the darkroom to

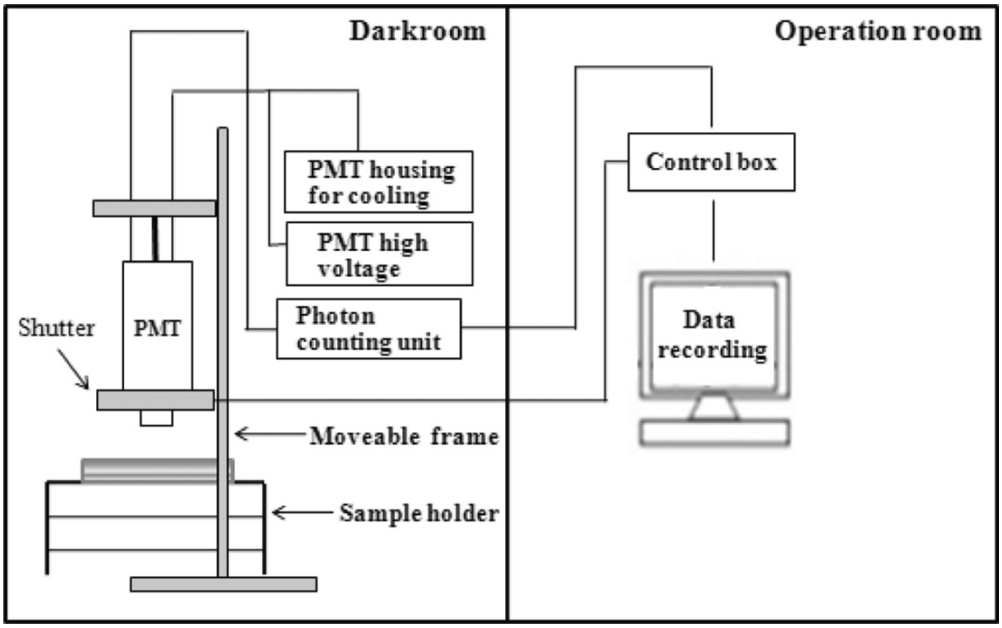

Fig. 1. The schematic representation of the biophoton detection system used in this study.

position the mice. During the measurement period, the temperature in the darkroom was controlled to 25 ± 1 °C.

2.2. Cell Culture

Human breast cancer cell line MDA-MB-231was purchased from the cell bank of Shanghai Institute of Cell Biology, Chinese Academy of Sciences and was maintained in DMEM supplemented with 10% FBS, 1% penicillin (100 U/mL)/streptomycin (100 μg/mL). Cells were incubated at 37 °C in a humidified atmosphere of 5% CO_2 in air as a monolayer culture in plastic culture plates (100 mm diameter) and routinely subcultured when 80% confluence was reached.

2.3. Athymic Nude Mice

Fifty healthy BALB/C female nude mice (5 weeks old) were acquired from Beijing HFK Bioscience Company. These mice were divided into three groups: experiment group ($n = 30$), control group ($n = 10$) and normal group ($n = 10$). All animal treatments were performed in accordance with international ethical guidelines and the National Institutes of Health Guide concerning the Care and Use of Laboratory Animals.

2.4. Subcutaneous Xenograft Transplantation

Before transplantation, MDA-MB-231 cells were maintained in a culture incubator as described above. The cells were trypsinized and suspended in physiological saline, and 5×10^6 cells in 0.15 mL physiological saline were injected subcutaneously into the right axillary of each nude mice (after being acclimated for 1 week) in the experimental group. For the control group, the right side of the mice was injected with 0.15 mL physiological saline. Following injection, the mice were maintained with a 12:12 h light:dark cycle with food and water available *ad libitum*.

2.5. Measurement Protocol

Each test was conducted between 2 p.m. and 4 p.m. to reduce the influence of diurnal rhythms. The following measurement protocol was used. **a):** The mice under test were placed on an ultraclean workbench with weak light and were weighed and anesthetized using 70% pentobarbital sodium (70 mg/kg). Following the injection, the mice were held in a cage for 5 min; then, each mouse was placed in a completely dark room with controlled temperature (25 ± 1 °C) and humidity (50%) for 20 min before measurement to eliminate delayed luminescence. **b):** The dark current (background noise) and standard light source (C^{14}) were measured to ensure the detection performance of the SPE-detection system and for follow-up data analysis. **c):** Subsequently, mice were placed on the sample holder with their limbs secured using black paper tape, and the SPE from the tumor transplantation site on the right side of the mouse and the same site on the left side were sequentially recorded. In each measurement process, the duration was10 min with agate time (interval time) of 0.05 s, and a total of 12,000 points were recorded. Each measurement took slightly >20 min. The next measurement was performed immediately after. **d):** Finally, the dark current and standard light source (C^{14}) were measured again.

The SPE measurement of the tumor transplantation sites started when the breast cancer cells were in the incubation period, and measurements were performed twice per week until tumors were obvious (as shown in Fig. 3).

2.6. Data Analysis

The statistical analysis of the SPE data was performed using SPSS 18.0 (SPSS, USA), and the data calculations and graphing were performed using Origin 9.1 and graphPad Prism 6.01. Cluster analysis was used to evaluate the discriminating power of the parameters and parameter combinations.

3. Results

3.1. The Performance of the Measurement System

Fig. 2 depicts the background (BG) signals and standard light source (C^{14}) at the same time (2:00 p.m.) on different days. It illustrated that the performance of the measurement system used in this study was stable.

3.2. The SPE Strength From the Body Surface of Mice in Each Group Throughout the Entire Growth Process of Breast Cancer

Fifty nude mice were used in this study: thirty in the experiment group, ten in the control group and ten in the normal group. In order to analyze the SPE from the body surface of mice in each group throughout the entire breast cancer growth process, SPE was initially measured when the breast cancer cells were in the incubation period and then twice per week until tumors were obvious. Fig. 3 displayed the growth stages of a mouse whose right axillary was injected with breast cancer cells. The detailed measurement protocol has been described in Section 2.5.

Among the thirty mice in the experimental group, twenty-two mice grew tumors (tumor mice group), while the other eight mice did not (tumor-free mice group). The SPE data from the three groups in the different growth stages of tumor xenograft (as shown in Fig. 3) were recorded, and the average strength (K) of the SPE was recorded as the mean ± variance. The results are presented in the Fig. 4 and these data has been corrected for their BG signals.

Fig. 4 showed that the SPE from the right and left side was equivalent in the normal ($p = 0.894$), control ($p = 0.373$) and tumor-free groups ($p = 0.572$), while a distinct difference was observed in the tumor group, no matter the diameter (r) of the tumors was <0.5 cm or greater than1.5 cm ($r < 0.5$ cm: $p = 0.021$; 1 cm < $r < 1.5$ cm: $p = 0.001$ and $r > 1.5$ cm: $p < 0.001$). In addition, SPE strength from both sides of the experimental group mice had a tendency to increase with increasing tumor size. The data in Fig. 4 suggested that physiological saline had no effect on SPE, but the *in vivo* growth of cancer cells did affect SPE. Fig. 4 also indicated that the SPE from the tumor transplantation sites tended to increase during the incubation period (before visible morphological changes) in the tumor mice group; however, because of the high variance of the average intensity, this change was not significant. In contrast, this phenomenon was not observed in the tumor-free mice.

3.3. The Ratio of SPE Strength Between the Right and Left Side of Mice in Each Group

To eliminate individual differences in SPE intensity and to further explore the characteristics of SPE during the tumor growth process, we calculated the ratio of the average SPE strength $((K_R - K_L) / (K_R + K_L))$ between the right (R) and left side (L) of the mice from each mouse. The results are presented in Fig. 5.

As shown in Fig. 5, using the ratio of SPE between the right and left sides of the mice reduced the individual differences in the same group and increased the difference between groups. Compared with the SPE strength analysis, the ratios of SPE between the right and left sides of the tumor mice were significantly higher than those from the tumor-free mice in the experiment group in the incubation period ($p < 0.001$). In addition, the SPE ratios of mice whose cancer was obvious were higher than those from tumor-free mice. However, the difference in ratios among the three cancer growth stages was small. The ratio was not clearly different among the normal group, control group and tumor-free mice in the experiment group. These indicated that the SPE ratios between the right side (tumor transplantation side) and left side

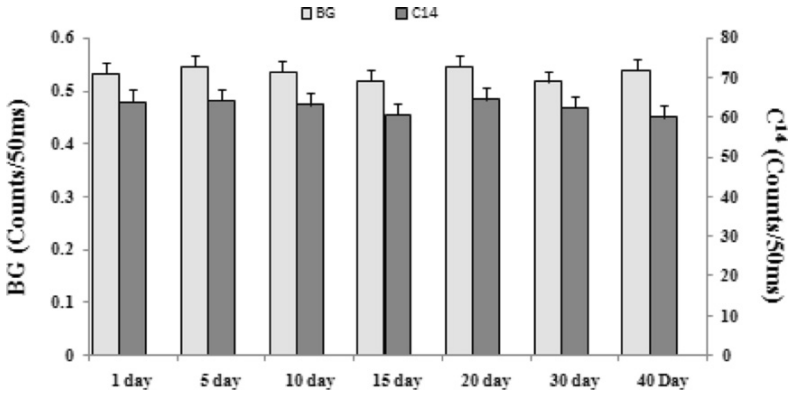

Fig. 2. The background signals and the standard light source at the same time (2:00 p.m.) on different days. BG, background; C^{14}, standard light source.

(normal side) of the mice could distinguish tumor mice from control mice in different tumor growth stages and could discriminate tumor mice from tumor-free mice before tumors were obvious, although tumors had been transplanted into all the mice.

3.4. Clustering Analysis to Evaluate the Discriminating Power of the Parameters Mentioned Above

Cluster analysis is a pattern recognition technique that is characterized by the use of resemblance or dissemblance measures between objects, that is to say, it can divide members into clusters sharing similar properties. Clustering analysis was introduced in this study to evaluate the power of the different parameters and parameter combinations mentioned above to distinguish tumor mice from the tumor-free mice, regardless of whether morphological characteristics were obvious. Because of the similarity characteristic of SPE between the normal and control mice, the parameters from control mice are used in this section.

Table 1 depicted the power of the parameters and parameter combinations to identify tumor mice from others in three tumor growth stages (incubation period, tumor diameter <0.5 cm and tumor diameter >1.5 cm), respectively. The clusters results were determined based on the parameter and parameter combination values at two sites of each subject. The clusters were identified by uppercase Roman numerals in brackets. The numbers of mice belonging to each group in the clusters were specified in Arabic numerals. The accuracy rates of strength-R, strength-L, ratio (R/L) and their combination to identify tumor mice from control mice in three different growth stages of tumor were displayed in Fig. 6.

The r represents the diameter of the tumor, L represents the left side, R represents the right side.

Data in Table 1 indicated that all the parameters from tumor-free mice were similar to those from control mice, and it was difficult to distinguish tumor-free and control mice in the tumor incubation period. However, there was a significant difference between the tumor mice and tumor-free mice or control mice, regardless of whether the tumor morphological characteristics were obvious. Although the signal strength from the right side (tumor transplantation side) of mice only had a 63.6% accuracy rate to identify tumor mice from tumor-free mice and control mice in the incubation period as shown in Fig. 6, the ratio(R/L) correctly identified 18 subjects in the tumor mice group, and the accuracy was 81.8%. This result proved that the ratio of the signal strength from both sides of nude mice could eliminate the individual differences in SPE intensity to a certain degree and could better respond to changes in biological information than the signal strength. To further increase the accuracy of the identification, we analyzed the parameter combination of signal strength-R, signal strength-L and ratio (R/L). As a result, three tumor mice were incorrectly identified, and the accuracy rate was 86.4% in the incubation period.

For nude mice with tumor diameter <0.5 cm, the accuracies of signal strength-R and ratio (R/L) were 72.7%, and 86.4%, respectively, while the accuracies of signal strength-L was 36.4%. The parameter combination of signal strength-R, signal strength-L and ratio (R/L) correctly identified 20 subjects in the tumor mice group (90.9%) and 8 subjects in the control mice group. These results were similar to the results in the tumor incubation period: the parameters from the tumor transplantation side of nude mice contained significant biological information that could be used to distinguish tumor mice from control mice, while the

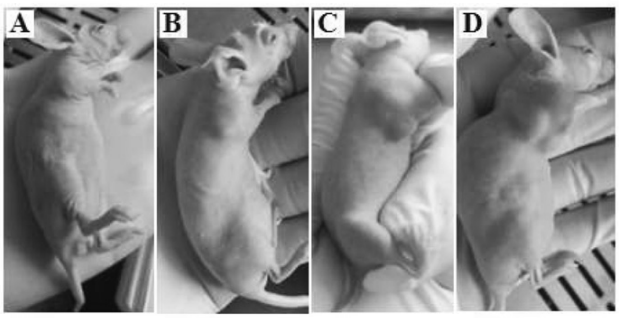

Fig. 3. The different growth stages of one mouse whose right axillary was injected with breast cancer cells. A: The incubation period of breast cancer; B: Tumor diameter <0.5 cm; C: Tumor diameter >1 cm and <1.5 cm; D: Tumor diameter >1.5 cm.

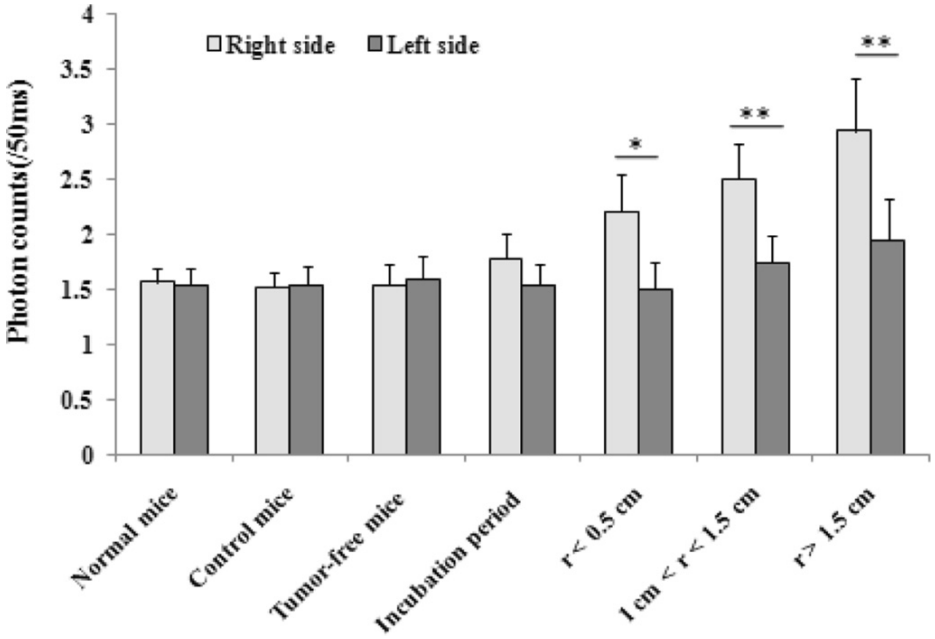

Fig. 4. SPE data from the two sides of mice in three groups. L, left side of mice; R, right side of mice; r, breast cancer tumor diameter.

parameters from the left side (without any operation) of nude mice could not. The parameter combination, which contained complementary information, had a higher accuracy than single parameters for correctly identifying tumor mice, regardless of whether the morphological characteristics were obvious.

For nude mice with tumor diameters larger than 1.5 cm, the accuracies of the signal strength-R and ratio (R/L) were 86.4% and 95.5%, respectively. In contrast to the two growth stages of tumors discussed above, the accuracies of the signal strength from the left side (without operation) of nude mice was 77.3%, which illustrated that with the increase of tumor volume, the SPE from the healthy side of tumor mice also changed and could be used as an indicator to distinguish tumor and control mice. The parameter combination of signal strength-R, signal strength-L and ratio (R/L) correctly identified all subjects in the tumor mice group (100%) and 9 subjects in control mice group (90%) in this growth stage.

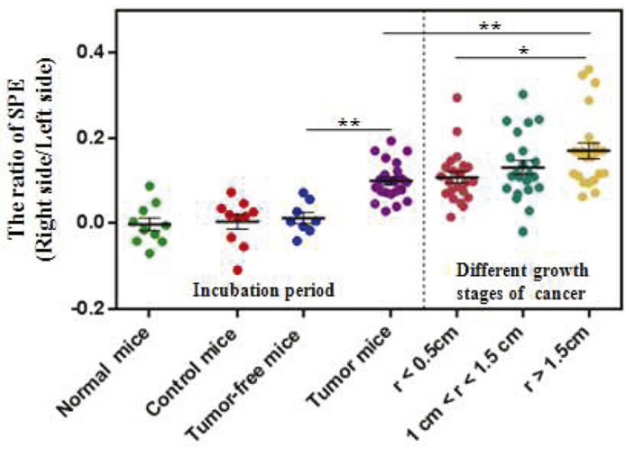

Fig. 5. The ratio of SPE $((K_R - K_L) / (K_R + K_L))$ between the right and left side of the mice from each group in the incubation period and different breast cancer growth stages in the tumor group. The r represents the diameter of the tumor. $^*p < 0.05$ and $^{**}p < 0.01$.

4. Discussion and Conclusion

SPE is an intrinsic attribute of biological systems, and studies have suggested that it is related to the oxidative metabolic processes of biological molecules [2,3,23,24]. The production of reactive oxygen species (ROS: $O_2^{\cdot-}$, $HO^{\cdot}$, H_2O_2, $^1O_2$) in metabolic processes plays a key role in SPE [24,25]. In animal cells, the generation of ROS is related to enzymatic reactions in mitochondria, the cytoplasm and peroxisomes, and cellular respiration in mitochondria is a main source [26–29]. ROS with high positive redox potential can oxidize a wide variety of cellular biomolecules, such as proteins, lipids, carbohydrate and nucleic acids, and initiate cascade reactions that are accompanied by the generation of electronically excited species, such as triplet-excited carbonyls ($^3R = O^*$), excited pigment (P^*) and singlet oxygen ($^1O_2$), resulting in photon emission [30–33]. Therefore, biophoton emission can be used to reflect the underlying metabolic processes in cells and indicate the physiological and pathological conditions of biological systems from an optical and non-invasive perspective.

In contrast to normal cells that primarily use oxidative phosphorylation for the production of energy under aerobic conditions and rely on glycolysis only when their oxygen supply is limited, cancer cell metabolism is often shifted from oxidative phosphorylation to glycolysis, even in the presence of sufficient amounts of oxygen as the primary generator of energy [34–38]. This switch of cellular metabolism, as well as a series of related biochemical reactions, may result in the changes in the levels of ROS in cancer cells. Indeed, many studies have reported that cancer cells show increased production of ROS compared with normal cells [39–42], and breast cancer is no exception. Several experimental investigations demonstrated that the rate of $O_2^{\cdot-}$ and H_2O_2 production was significantly higher in breast cancer patients than the controls [43,44]. Considering the close relationship between SPE and ROS described above, the SPE from cancer cells or bodies may be notably different from that of the controls. Accordingly, the SPE associated with the cellular metabolism may be a powerful biophysical indicator for tumor analysis [45]. The difference in biophoton emission between cancer cells and normal cells associated with the level of ROS has been confirmed by researchers [9,10,46,47]. However, the characteristics of biophoton emission from the surface of a tumor body has not been thoroughly studied.

Table 1
Clustering result of nude mice based on the value of the parameters or parameter combinations at two sites of each subject. The number of clusters varies from 2 to 3 for different parameters and parameter combinations.

The states of tumor	Parameters	Tumor mice group ($n = 22$)	Tumor-free mice group($n = 8$)	Control mice ($n = 10$)
Incubation period	1) Signal strength-R	14(I) + 7(II) +1(III)	2(I) + 6(II)	1(I) + 9(II)
	2) Signal strength-L		9(I) + 10(II) + 3(III)	6(I) + 2(II)
	8(I) + 2(II)			
	3) Ratio (R/L)	18(I) + 4(II)	1(I) + 7(II)	1(I) + 9(II)
1) + 2) + 3)	19(I) + 3(II)	2(I) + 6(II)	10(II)	
$r < 0.5$ cm	1) Signal strength-R	16(I) + 6(II)	–	1(I) + 9(II)
	2) Signal strength-L	8(I) + 9(II) + 5(III)	–	5(I) + 5(II)
	3) Ratio(R/L)	19(I) + 3(II)	–	4(I) + 6(II)
	1) + 2) + 3)	20(I) + 2(II)	–	2(I) + 8(II)
$r > 1.5$ cm	1) Signal strength-R	19(I) + 3(II)	–	10(II)
	2) Signal strength-L	17(I) + 5(II)	–	1(I) + 9(II)
	3) Ratio(R/L)		17(I) + 1(II) + 4(III)	–
	1(I) + 9(II)			
1) + 2) + 3)	22(I)	–	9(II) + 1(I)	

In the present study, we investigated the characteristics of SPE from the body surface of a human breast cancer-bearing nude mouse model during the entire breast cancer growth process to prove that SPE from the body surface could be used as a biophysical indicator for tumor analysis that is not limited to cancer cells or tissues. This point was verified by our data. SPE from the body surface could significantly distinguish tumor mice from the controls when tumors were obvious and when there were no obvious morphological changes, although the accuracy was relatively low. These experimental results indicated that the SPE from the body surface was sensitive to changes in physiological and pathological conditions *in vivo* and could be used as a meaningful biophysical indicator for tumor analysis, at least for breast cancer, even though the cancer was in its primary stage. Considering the disadvantages of the current imaging diagnostic methods for the early screening of breast cancer described in the introduction, this SPE detection method can be a non-invasive and powerful detection method for the preliminary screening of breast cancer or supplementary diagnostic aid for early diagnosis.

Another discovery of this study was that the discrepancies of the SPE parameters between the tumor mice and the controls gradually increased with the increase of tumor size. As breast cancer developed ($r > 1.5$ cm in this paper), the SPE from the healthy side of tumor mice also changed (as shown in Fig. 6: signal strength-L). Although the precise mechanism was not clear, this phenomenon may be associated with a complex oxidative metabolic process controlled by multiple genes and proteins, involving a number of physiological and biochemical reactions and energy transition changes in the biological system. This process will lead to differences in photon emission.

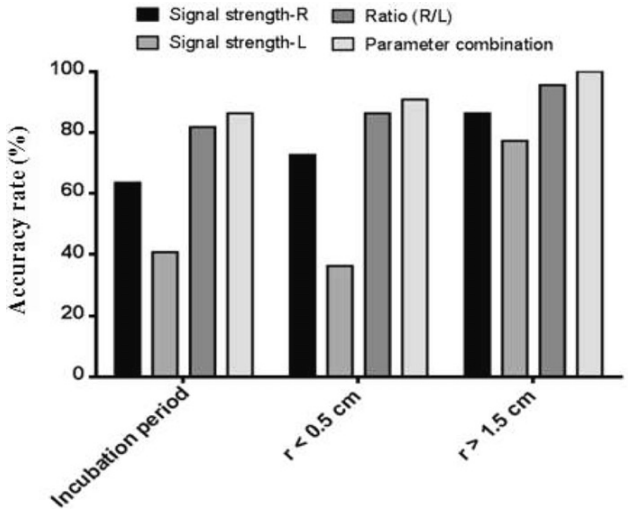

Fig. 6. Accuracy rates of strength-R, strength-L, ratio (R/L) and their combination to identify tumor mice from control mice. L represents the left side of the nude mouse, R represents the right side of the nude mouse, r represents the diameter of the tumor.

In conclusion, we reported the characteristics of SPE from the body surface of a human breast cancer-bearing nude mouse model throughout the entire growth process of breast cancer using a sensitive PMT. Our data showed that the SPE from the body surface could significantly distinguish tumor mice from healthy controls, regardless of whether the morphological change at the lesion site was obvious. Our data also illustrated that the SPE from the body surface of the lesion site was sensitive to changes in tumor size. In addition, the parameters of signal strength-R, signal strength-L and ratio (R/L) could be used to reflect the SPE characteristics, and the discriminating power of these parameters and parameter combination could be evaluated by cluster analysis. Although the precise mechanism of SPE from the body surface of nude mice has not been elucidated fully, these results indicated that the SPE from the body surface contained abundant metabolic information and was closely related to the breast cancer growth. The SPE of many more subjects and different types of breast diseases need to be studied, and further accumulation of data could lead to the construction of a multi-level database to develop novel diagnostic tools for breast diseases.

Acknowledgments

This work is funded by grants from the National Natural Science Foundation of China (No. 81273997), Ministry of Science and Technology of China (2014DFA30380) and Shandong Provincial Natural Science Foundation, China (ZR2015HQ016). We thank all the individuals who participated in these studies and all the researchers, technicians and administrative staff who have enabled this work. We would like to acknowledge Dr. Eduard Van Wijk (Meluna Research), Mei Wang and Dr. Yu Yan for supervising the construction of the equipment and technical assistance.

References

[1] F.A. Popp, Properties of biophotons and their theoretical implications, Indian J. Exp. Biol. 41 (2003) 391–402.
[2] J. Sławinski, Biophotons from stressed and dying organisms: toxicological aspects, Indian J. Exp. Biol. 41 (2003) 483–493.
[3] W.R. Van, E.P. Van Wijk, F.A. Wiegant, J. Ives, Free radicals and low-level photon emission in human pathogenesis: state of the art, Indian J. Exp. Biol. 46 (2008) 273–309.
[4] E. Bertogna, J. Bezerra, E. Conforti, C.M. Gallep, Acute stress in seedlings detected by ultra-weak photon emission, J. Photochem. Photobiol. B. 118 (2013) 74–76.
[5] K. Kato, H. Iyozumi, C. Kageyama, H. Inagaki, A. Yamaguchi, H. Nukui, Application of ultra-weak photon emission measurements in agriculture, J. Photochem. Photobiol. B. 139 (2014) 54–62.

[6] M. Hossu, M. Lun, C. Wei, Nonlinear enhancement of spontaneous biophoton emission of sweet potato by silver nanoparticles, J. Photochem. Photobiol. B. 99 (2010) 44–48.
[7] J. Pang, J. Fu, M. Yang, X. Zhao, E.V. Wijk, M. Wang, H. Fan, J. Han, Correlation between the different therapeutic properties of Chinese medicinal herbs and delayed luminescence, Luminescence 31 (2015) 323–327.
[8] M. Iranifam, Analytical applications of chemiluminescence methods for cancer detection and therapy, TrAC Trends Anal. Chem. 59 (2014) 156–183.
[9] H.W. Kim, S.B. Sim, C.K. Kim, J. Kim, C. Choi, H. You, K.S. Soh, Spontaneous photon emission and delayed luminescence of two types of human lung cancer tissues: Adenocarcinoma and Squamous cell carcinoma, Cancer Lett. 229 (2005) 283–289.
[10] F. Musumeci, G. Privitera, A. Scordino, S. Tudisco, C.L. Presti, L.A. Applegate, H.J. Niggli, Discrimination between normal and cancer cells by using spectral analysis of delayed luminescence, Appl. Phys. Lett. 86 (2005) 153902.
[11] M. Takeda, M. Kobayashi, M. Takayama, S. Suzuki, T. Ishida, K. Ohnuki, T. Moriya, N. Ohuchi, Biophoton detection as a novel technique for cancer imaging, Cancer Sci. 95 (2004) 656–661.
[12] P. Chen, L. Zhang, F. Zhang, J.T. Liu, H. Bai, G.Q. Tang, L. Lin, Spectral discrimination between normal and leukemic human sera using delayed luminescence, Biomedical Opt. Express 3 (2012) 1787–1792.
[13] L. Lanzanò, A. Scordino, S. Privitera, S. Tudisco, F. Musumeci, Spectral analysis of delayed luminescence from human skin as a possible non-invasive diagnostic tool, Eur. Biophys. J. 36 (2007) 823–829.
[14] W.E. Van, M. Kobayashi, W.R. Van, G.J. Van, Imaging of ultra-weak photon emission in a rheumatoid arthritis mouse model, PLoS One 8 (2013), e84579. .
[15] M. Yang, J. Pang, J. Liu, Y. Liu, H. Fan, J. Han, Spectral discrimination between healthy people and cold patients using spontaneous photon emission, Biomedical Opt. Express 6 (2015) 1331–1339.
[16] X.L. Zhao, J.X. Han, The connotation of the Quantum Traditional Chinese Medicine and the exploration of its experimental technology system for diagnosis, Drug Discov. Ther. 7 (2013) 225–232.
[17] P.A. Carney, C.J. Kasales, A.N.A. Tosteson, J.E. Weiss, M.E. Goodrich, S.P. Poplack, W.S. Wells, L. Titus-Ernstoff, Likelihood of additional work-up among women undergoing routine screening mammography: the impact of age, breast density, and hormone therapy use, Prev. Med. 39 (2004) 48–55.
[18] T. Hata, H. Takahashi, K. Watanabe, M. Takahashi, K. Taguchi, T. Itoh, S. Todo, Magnetic resonance imaging for preoperative evaluation of breast cancer: a comparative study with mammography and ultrasonography, J. Am. Coll. Surg. 198 (2004) 190–197.
[19] W.H. Hindle, L. Davis, D. Wright, Clinical value of mammography for symptomatic women 35 years of age and younger, Am. J. Obstet. Gynecol. 180 (1999) 1484–1490.
[20] S. Kala, C. Pantola, A. Agarwal, A. Pradhan, S. Thakur, Optical spectroscopy: a promising diagnostic tool for breast lesions, Journal of Clinical & Diagnostic Research 5 (2011) 1574–1577.
[21] M. Takeda, Y. Tanno, M. Kobayashi, M. Usa, N. Ohuchi, S. Satomi, H. Inaba, A novel method of assessing carcinoma cell proliferation by biophoton emission, Cancer Lett. 127 (1998) 155–160.
[22] J. Kim, J. Lim, H. Kim, S. Ahn, S.B. Sim, K.S. Soh, Scanning spontaneous photon emission from transplanted ovarian tumor of mice using a photomultiplier tube, Electromagn. Biol. Med. 25 (2006) 97–102.
[23] A. Rastogi, P. Pospísil, Spontaneous ultraweak photon emission imaging of oxidative metabolic processes in human skin: effect of molecular oxygen and antioxidant defense system, J. Biomed. Opt. 16 (2011) 096005.
[24] P. Pospíšil, A. Prasad, M. Rác, Role of reactive oxygen species in ultra-weak photon emission in biological systems, J. Photochem. Photobiol. B. 139 (2014) 11–23.
[25] A. Rastogi, P. Pospíšil, Effect of exogenous hydrogen peroxide on biophoton emission from radish root cells, Plant Physiol. Biochem. 48 (2010) 117–123.
[26] D. Han, E. Williams, E. Cadenas, Mitochondrial respiratory chain-dependent generation of superoxide anion and its release into the intermembrane space, Biochem. J. 353 (2001) 411–416.
[27] A.J. Lambert, M.D. Brand, Superoxide production by NADH:ubiquinone oxidoreductase (complex I) depends on the pH gradient across the mitochondrial inner membrane, Biochem. J. 382 (2004) 511–517.
[28] J. Bylund, H. Björnsdottir, M. Sundqvist, A. Karlsson, C. Dahlgren, Measurement of respiratory burst products, released or retained, during activation of professional phagocytes, Methods Mol. Biol. 1124 (2014) 321–338.
[29] V.N. Daithankar, W. Wang, J.R. Trujillo, C. Thorpe, Flavin-linked Erv-family sulfhydryl oxidases release superoxide anion during catalytic turnover, Biochemistry 51 (2012) 265–272.
[30] S. Miyamoto, G.E. Ronsein, F.M. Prado, M. Uemi, T.C. Corrêa, I.N. Toma, A. Bertolucci, M.C.B. Oliveira, F.D. Motta, M.H.G. Medeiros, Biological hydroperoxides and singlet molecular oxygen generation, IUBMB Life 59 (2007) 322–331.
[31] G.F. Fedorova, A.V. Trofimov, R.F. Vasil'Ev, T.L. Veprintsev, Peroxy-radical-mediated chemiluminescence: mechanistic diversity and fundamentals for antioxidant assay, ChemInform 38 (2007) 163–215.
[32] S. Birtic, B. Ksas, B. Genty, M.J. Mueller, C. Triantaphylidès, M. Havaux, Using spontaneous photon emission to image lipid oxidation patterns in plant tissues, Plant J. 67 (2011) 1103–1115.
[33] T. Nguyen, D. Brunson, C.L. Crespi, B.W. Penman, J.S. Wishnok, S.R. Tannenbaum, DNA damage and mutation in human cells exposed to nitric oxide in vitro, Proc. Natl. Acad. Sci. U S A. 89 (1992) 3030–3034.
[34] O. Warburg, On the origin of cancer cell, Science 123 (1956) 309–314.
[35] D.Q. Yang, D.M. Freund, B.R. Harris, D. Wang, M.P. Cleary, A.D. Hegeman, Measuring relative utilization of aerobic glycolysis in breast cancer cells by positional isotopic discrimination, FEBS Lett. 590 (2016) 3179–3187.
[36] C. Xintaropoulou, C. Ward, A. Wise, H. Marston, A. Turnbull, S.P. Langdon, A comparative analysis of inhibitors of the glycolysis pathway in breast and ovarian cancer cell line models, Oncotarget 6 (2015) 25677–25695.
[37] M.G. Vander Heiden, L.C. Cantley, C.B. Thompson, Understanding the Warburg effect: the metabolic requirements of cell proliferation, Science 324 (2009) 1029–1033.
[38] P.P. Hsu, D.M. Sabatini, Cancer cell metabolism: Warburg and beyond, Cell 134 (2008) 703–707.
[39] T.P. Szatrowski, C.F. Nathan, Production of large amounts of hydrogen peroxide by human tumor cells, Cancer Res. 51 (1991) 794–798.
[40] M.D. Evans, M. Dizdaroglu, M.S. Cooke, Oxidative DNA damage and disease: induction, repair and significance, Mutat. Res. 567 (2004) 1–61.
[41] H. Pelicano, D. Carney, H. Peng, ROS stress in cancer cells and therapeutic implications, Durg Resist. Updat. 7 (2004) 97–110.
[42] J.L. Quiles, A.J. Farquharson, D.K. Simpson, I. Grant, K.W. Wahle, Olive oil phenolics: effects on DNA oxidation and redox enzyme mRNA in prostate cells, Br. J. Nutr. 88 (2002) 225–234 (discussion 223–224).
[43] L. Vera-Ramirez, P. Sanchez-Rovira, M.C. Ramirez-Tortosa, C.L. Ramirez-Tortosa, S. Granados-Principal, J.A. Lorente, J.L. Quiles, Free radicals in breast carcinogenesis, breast cancer progression and cancer stem cells. Biological bases to develop oxidative-based therapies, Crit. Rev. Oncol. Hematol. 80 (2011) 347–368.
[44] G. Ray, S. Batra, N.K. Shukla, S. Deo, V. Raina, S. Ashok, S.A. Husain, Lipid peroxidation, free radical production and antioxidant status in breast cancer, Breast Cancer Res. Treat. 59 (2000) 163–170.
[45] A. Walsh, R.S. Cook, B. Rexer, C.L. Arteaga, M.C. Skala, Optical imaging of metabolism in HER2 overexpressing breast cancer cells, Biomed. Opt. Express 3 (2012) 75–85.
[46] F. Musumecia, L.A. Applegatec, G. Priviteraa, A. Scordinoa, Spectral analysis of laser-induced ultraweak delayed luminescence in cultured normal and tumor human cells: temperature dependence, J. Photochem. Photobiol. B. 79 (2005) 93–99.
[47] M. Takeda, M. Kobayashi, M. Takayama, S. Suzuki, T. Ishida, K. Ohnuki, T. Moriya, N. Ohuchi, Biophoton detection as a novel technique for cancer imaging, Cancer Sci. 95 (2004) 656–661.